



Use of temporal/seasonal- and size-dependent bioaerosol data to characterize the contribution of outdoor fungi to residential exposures

Chung-Min Liao*, Wen-Chang Luo

Ecotoxicological Modeling Center, Department of Bioenvironmental Systems Engineering, National Taiwan University, Taipei, Taiwan 10617, ROC

Received 18 April 2004; accepted 1 December 2004
Available online 29 January 2005

Abstract

With the use of published temporal/seasonal and particle size distribution of outdoor bioaerosol data and meteorological information in the subtropical climate, we characterized the airborne fungal concentration indoor/outdoor/personal exposure relationships in a wind-induced naturally ventilated residence. We applied a size-dependent indoor/outdoor ratio model coupled with a compartmental lung model based on a hygroscopic growth factor as a function of relative humidity on aerodynamic diameter and concentration of fungal spores. The higher indoor airborne fungal concentrations occurred in early morning and late afternoon in which median values were 699.29 and 626.20 CFU m⁻³ in summer as well as 138.71 and 99.01 CFU m⁻³ in winter, respectively, at 2 am and 8 pm. In the absence of indoor sources, summer has higher mean indoor/outdoor ratios of airborne fungal concentration (0.29–0.58) than that in winter (0.12–0.16). Lung region of extrathoracic (ET) has higher fungal concentration lung/indoor ratios (0.7–0.8) than that in bronchial (BB; 0.41–0.60), bronchiolar (bb; 0.12–0.40), and alveolar-interstitial (AI; 0.01–0.24) regions. The highest airborne fungal deposition dose (95th-percentile is 4600 CFU) occurred in 11 pm–5 am in region AI in that the 95th-percentile fungal deposition rate was 0.22 CFU s⁻¹.

© 2004 Elsevier B.V. All rights reserved.

Keywords: Airborne fungus; Bioaerosol; Hygroscopic; Humidity; Inhalation dose; Natural ventilation

1. Introduction

House dust mite and fungus allergen are observed to be the predominant allergens in Taiwan (Kuo and Li,

1994; Li et al., 1996; Wu et al., 2000). Su et al. (2001), Huang et al. (2002), and Su et al. (2002) in their epidemiological studies indicated that fungal spores of ambient air are associated with many health effects, such as increased respiratory symptoms, decreased lung function, increased hospital emergency admissions and respiratory and cardiovascular mortality. Reponon et al. (1996) reported that human exposure to

* Corresponding author. Tel.: +886 2 2363 4512; fax: +886 2 2362 6433.

E-mail address: cmliao@ntu.edu.tw (C.-M. Liao).

airborne fungal spores might cause adverse health effects, especially respiratory symptoms.

Pasanen et al. (1991), Johnson et al. (1999), Hyvärinen et al. (2001), and Meklin et al. (2002) pointed out that aerodynamic sizes of the spores are typical for specific microorganism species, but may also vary due to physical conditions of the indoor environments such as air humidity. The hygroscopic growth, which means increase of a particle diameter by condensation or water absorption, influences the deposition and kinetic of aerosol. Some studies performed at air relative humidity of 12–73% (Pasanen et al., 1991) and 40–95% (Madelin and Johnson, 1992) had concluded that airborne fungal spores are hygroscopic. Burge et al. (1995) indicated that the extent of airborne fungi is closely related to indoor relative humidity (RH), below 30% RH little interior mold growth usually occurs, while above 70% RH conditions may be optimal for fungal growth. The hygroscopic of airborne fungi may significantly affect their aerodynamic diameter, and thus change their deposition pattern in indoor environment. Law et al. (2001) also indicated that the background fungal concentration was found to have strong correlation with the indoor RH level provided that the RH level could be maintained for a certain period of time.

As most time of 70–90% is spend indoors, information on the indoor and outdoor relationships of airborne fungal concentrations is important. Burge et al. (1995) pointed that the air in almost all indoor environments also contains fungal spores, and the environmental factors that influence indoor airborne fungal concentrations include outdoor concentrations, type and rate of ventilation, and indoor moisture levels. The main source of airborne fungi in indoor air is usually outdoor air. (Wu et al., 2000; Su et al., 2001) Huang et al. (2002) indicated that the distribution of airborne fungi appeared to be associated with seasonal changes in Taiwan region in that the concentrations of airborne fungi were higher in summer at some work environment and residence than that in winter. Therefore, to best document the actual environmental exposures of fungal spores, the effects of seasonality and temporality on the distribution of microorganisms should be considered.

Several studies have estimated deposition rates indoors, although there is considerable variability in

the methods used and types of particle examined (Crump and Seinfeld, 1981; Lai and Nazaroff, 2000). Depending on the flow regime, different models have been proposed for particle deposition in a ventilated airspace. Aerodynamic equivalent diameter (AED) particle size determines particle motion including settling under gravity, resuspension, and transport by air movement (Hinds, 1999). although diffusiophoresis and thermophoresis can be neglected, Brownian and turbulent diffusion, sedimentation, and laminar as well as convective flow exist to varying degrees and lead to fungi deposition onto walls and other surfaces. In the present work we adopted a mathematical model derived by Crump and Seinfeld (1981) for the rate of airborne fungi deposition in a turbulence mixing enclosure of arbitrary shape under the assumption of homogeneous turbulent near the surfaces.

Apart from deposition, independently measuring the penetration efficiencies of particles is very difficult. In our present study, we assumed that the penetration of particles is totally induced by wind-induced naturally ventilation. Natural ventilation is widely used in Taiwanese residences with the advantages of saving energy, expense, and installation time in that houses are controlled by natural convection to remove excessive heat and moisture. The mechanism of natural ventilation depends on wind effects, thermal buoyancy and the combination of both wind and buoyancy forces. Wind speed and wind direction are the dominant factors for wind-induced effects (Yu et al., 2002). The characteristics of openings affect natural ventilation efficiency with the arrangement, location, and control of ventilation openings to achieve a desired ventilation rate and good distribution of ventilation air through the buildings.

A complete particle exposure model for human respiratory tract (HRT) includes airflow dynamic, physiological, lung morphological, and dose cumulated submodels. Numerous mathematical models for predicting particulate matter (PM) deposition in the HRT have been developed over the years (ICRP, 1994; Lazaridis et al., 2001). In this present study, we employed an approach based on the concept of applying compartmental modeling to the human lung anatomy incorporated with the ICRP66 recommended model (ICRP, 1994). Numerous compartmental models have been proposed, differing in the representation

of the tracheo-bronchial tree, the breathing physiology and resulting airflow, and the expressions used for calculating PM deposition efficiencies (Koblinger and Hofmann, 1990). The main features of PM-bound fungal spores deposition mechanisms in lung include turbulent and Brownian diffusion, inertial impaction, interception, gravitational settling, and clearance as suggested by ICRP66 (ICRP, 1994).

The objectives of this paper were therefore set to predict the airborne fungi indoor/outdoor/personal

exposure relationships with variations of seasonal and temporal and meteorological effects focusing on building characteristics, i.e., wind-induced natural ventilation and their size-dependent effects on indoor airborne fungal levels. We predicted the temporal/seasonal variations of size-dependent indoor/outdoor (I/O) ratios of airborne fungal concentrations and characterized the contribution of outdoor fungi to residential exposures for urban naturally ventilated homes.

2. Materials and methods

2.1. Reanalysis of outdoor fungal spores data

Lin and Li (1996) have conducted a detailed field investigation to evaluate size characteristics of airborne fungal spores in Taipei region by Andersen six-stage viable sampler in summer and winter. The field samples were collected at a 6-h interval at 8 am, 2 pm, 8 pm, and 2 am for consecutive 7 days. Lin and Li (1996) indicated that the highest number of fungal spores occurred at nighttime, with a value above 1700 CFU m⁻³, yet decreased to a level of 450–600 CFU m⁻³ at daytime in that larger numbers of fungal spores isolated were found to be in the size range of 2.1–3.3 μm AED with a geometric mean diameter (GMD) in the size range of 1.96–3.40 μm AED.

We adopted their research results as our major database to appraise the temporal/seasonal variations of size-dependent airborne fungi indoor/outdoor/personal exposure relationships in a wind-induced naturally ventilated airspace. We used box and whisker plots to demonstrate the seasonal variation of wind speed, wind direction, and temperature, as well as temporal/seasonal variations of indoor/outdoor RH and outdoor airborne fungal concentrations data (Fig. 1), in that indoor RH was estimated via psychrometric processes with the known outdoor temperature and RH.

We used the Kolmogorov–Smirnov (K-S) statistics to optimize the goodness-of-fit of distribution, suggesting the lognormal distribution fits the observed data. We used the lognormal distribution model to fit data of size distributions of total airborne fungal concentration, resulting in GMDs of 2.28, 2.76, 3.09, and 2.18 μm AED at 2 am, 8 am, 2 pm, and 8 pm, respectively, with geometric standard deviation (GSD) 1.45–1.80 in summer; whereas GMDs of 2.62, 3.01, 3.16, and 2.36 μm AED at 2 am, 8 am, 2 pm, and 8 pm, respectively, with GSD 1.62–1.72 in winter (Fig. 2).

2.2. Fungal spores I/O ratio model

We employed a well-developed indoor/outdoor ratio model (Abt et al., 2000; Riley et al., 2002; Liao et al., 2003) to calculate the uncorrelated size-specific, time-averaged airborne fungal concentrations I/O ratio,

$$\frac{C_I(k)}{C_O(k)} = \frac{\lambda_n}{\lambda_n + \lambda_d(k)}, \quad k = 1, 2, \dots, N, \quad (1)$$

where $C_I(k, t)$ is the time-dependent indoor concentration of fungal spores in the k th size range (CFU m⁻³); $C_O(k, t)$ is the time-dependent outdoor concentration of fungal spores in the k th size range (CFU m⁻³); λ_n is the air exchange rate of natural ventilation through open windows and doors (h⁻¹) in which $\lambda_n = Q_n/V$, Q_n is the natural ventilation rate (m³ h⁻¹); V is the air volume (m³); $\lambda_d(k)$ is the deposition rate of indoor fungal spores

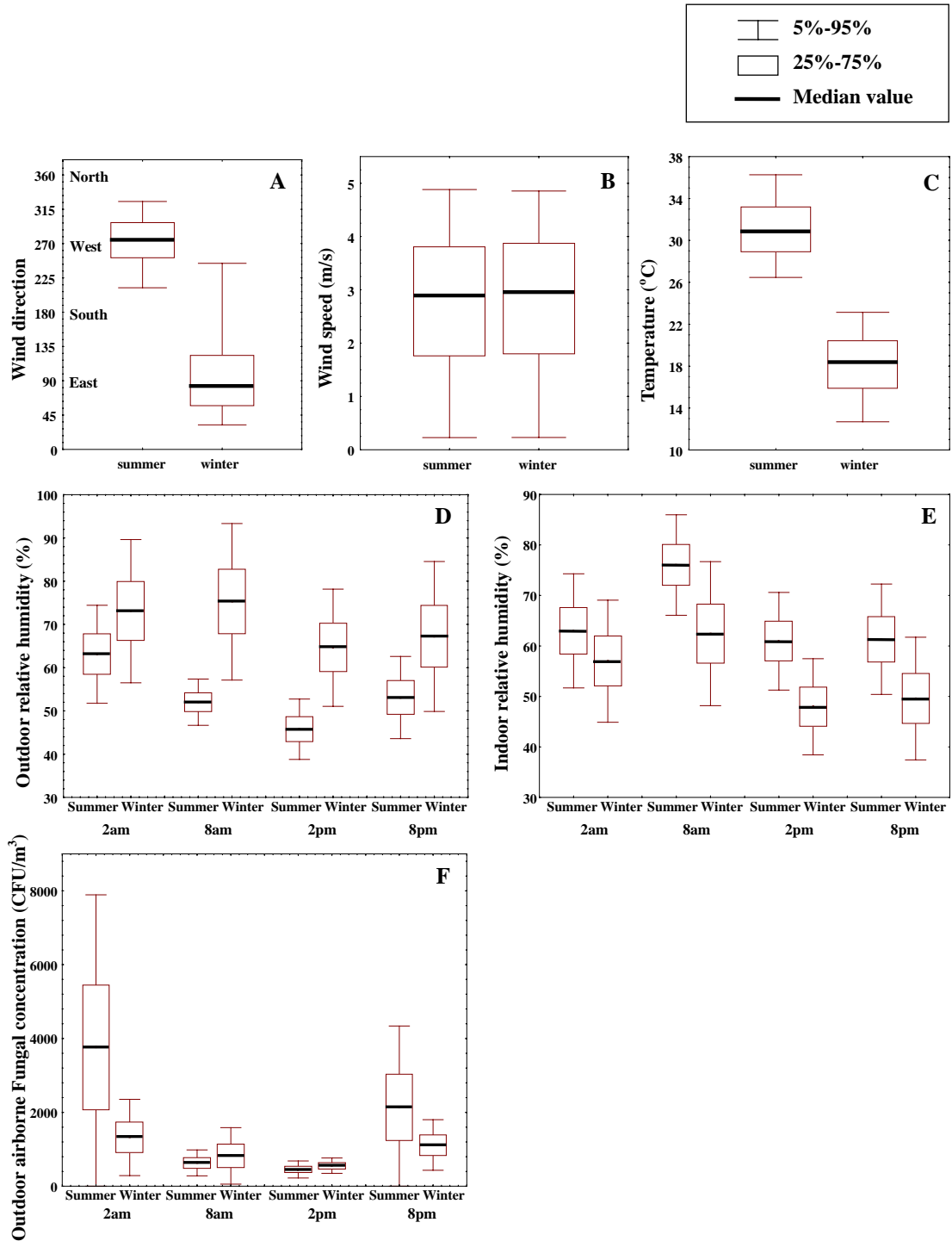


Fig. 1. Box and whisker plot representations of seasonal variation on (A) wind direction, (B) wind speed, (C) temperature, and temporal/seasonal variations on (D) outdoor relative humidity, (E) indoor relative humidity, and (F) outdoor airborne fungal concentrations analyzed from the measured data by Lin and Li (1996).

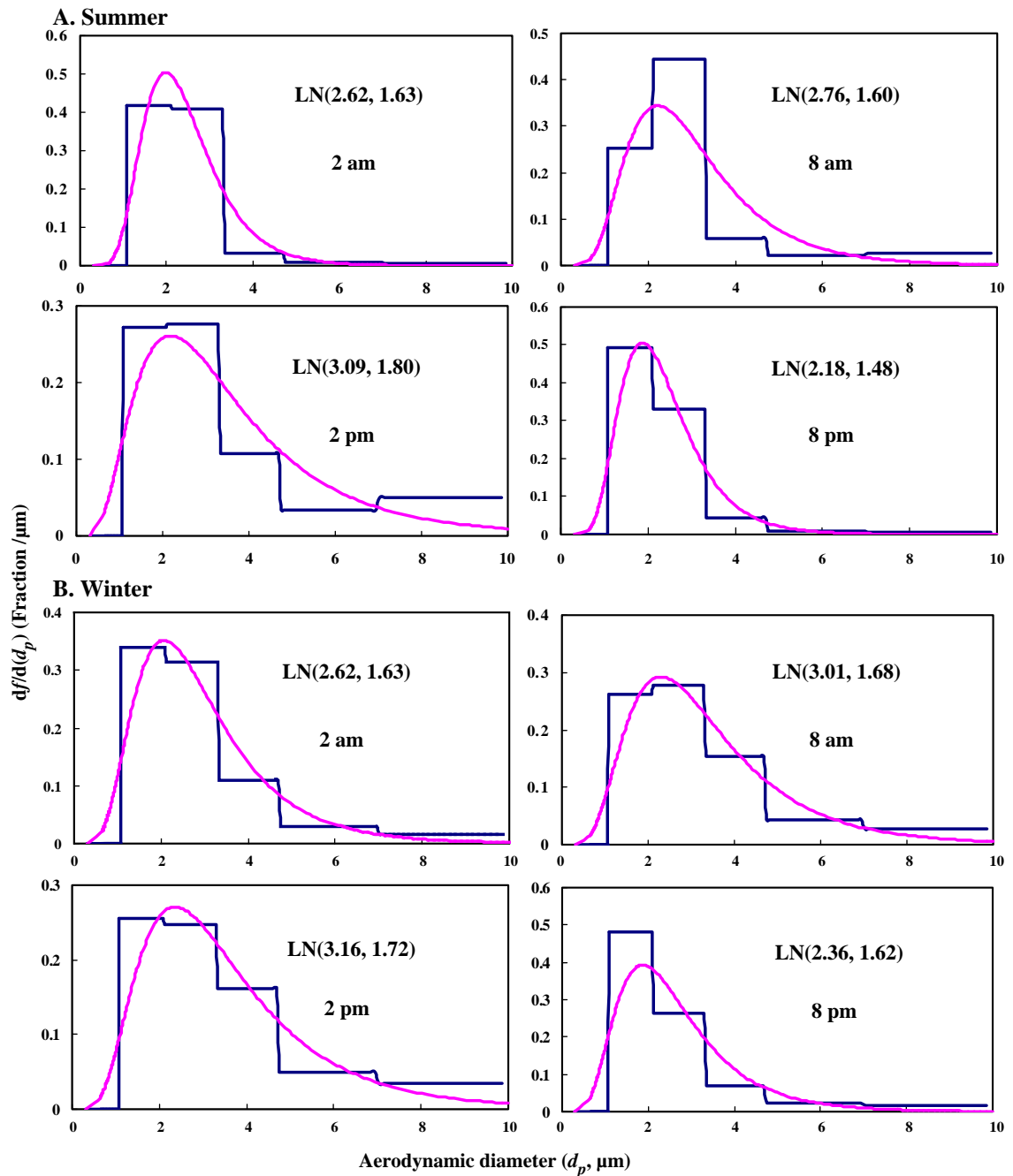


Fig. 2. Temporal size distribution of total airborne fungi in (A) summer and in (B) winter. The observed data are denoted by bar charts and the fitted model is represented by curve line in which $\text{LN}(a, b)$ gives the lognormal distribution with $\text{gmd } a \text{ } \mu\text{m}$ and $\text{gsd } b$.

due to Brownian and turbulent diffusive deposition and gravitational sedimentation in the k th size range (h^{-1}); k is the size range number; and N is assigned to be the end point number for a k th size range, d_k and d_{k+1} . The particles are divided into geometrically equal sized bins in the size range of interest. The concentration of fungal

spores is assumed to be a constant AED within each bin size. The end points, d_k and d_{k+1} , of the k th bin size are considered to be equal to the geometric mean of the end points of the bin size as, $d_k = d_{\min} + [(d_{\max} - d_{\min}) / (k - 1)](N - 1)$, where particles smaller than d_{\min} (the minimum diameter) are considered to be the finest, and d_{\max} is the largest particle size of interest. Eq. (1) is developed based on the principle of mass balance under an isothermal condition in that resuspension, coagulation of particles, and phase change processes are neglected.

The natural ventilation rate (Q_n) depends on the effect of wind moving through openings. We followed a commonly used equation $Q_n = EAV_w$ to predict the flow through a sidewall opening where E is the opening effectiveness (dimensionless), A is the area of inlet opening (m^2), and V_w is the wind speed ($m\ s^{-1}$). We employed an opening effectiveness model (Yu et al., 2002) depending on wind speed/direction and window/door openings to estimate the air exchange rates. Table 1 summarizes the essential parameters used to estimate the opening effectiveness for building type considered in this work.

2.3. Effects of relative humidity on fungal spores

We developed a RH–AED growth coefficient profile and a RH–concentration profile for airborne fungi to correct the proposed I/O ratio model presented in Eq. (1). We applied the research findings obtained from Reponon et al. (1996), Johnson et al. (1999), and Lee et al. (2002) to derive a RH–AED profile so as to determine the specific growth coefficient versus AED of airborne fungi (Fig. 3A). Fig. 3A indicates that specific growth coefficient (g , dimensionless) and RH (%) has a linear relationship as: $g(RH) = 0.0027\ RH + 0.84$ ($r^2 = 0.80$, $p < 0.05$) for RH ranging from 10% to 100%. Based on Fig. 3A, we could obtain a corrected factor for AED of airborne fungi due to RH changes as:

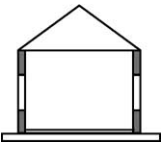
$$RH_{d_p} = \frac{g(RH_i)}{g(RH_o)}, \tag{2}$$

where RH_{d_p} is the AED corrected factor due to RH changes, $g(RH_i)$ is the specific growth coefficient due to indoor RH (RH_i , %), and $g(RH_o)$ is the specific growth coefficient due to outdoor RH (RH_o , %). Thus, AED-corrected I/O ratio model in Eq. (1) due to RH changes can be expressed as

$$\frac{C_I(k')}{C_O(k')} = \frac{\lambda_n}{\lambda_n + \lambda_d(k')}, \tag{3}$$

where $k' = k \times RH_{d_p}$ is the AED-corrected size range number.

Table 1
Parameters used to determine opening effectiveness for building type considered^a

Building type ^b	V	h_o/l_o	θ	ϕ	Median wind speed ($m\ s^{-1}$) (median wind direction) ^c		Opening effectiveness E_{sp} ^d	
					Summer	Winter	Summer	Winter
						$8 \times 8 \times 4 = 256$	2/3	30°

^a $V = l \times w \times h = \text{volume}$ (m^3), $h_o/l_o = \text{height to length ratio of inlet opening}$, $\theta = \text{roof slope angle}$, $\phi = \text{mean incidence of wind angles}$.

^b Surface area-to-volume ratio is $1.0\ m^{-1}$ and the area of inlet opening $A = 1.5\ m^2$.

^c See Fig. 1.

^d $E_{SP} = 7.44 \times (0.2Re)^{-0.35} \times (4h_o/l_o)^{0.10} \times (\sin\phi)^{0.75} \times (\sin\theta)^{-0.15}$ (Yu et al., 2002).

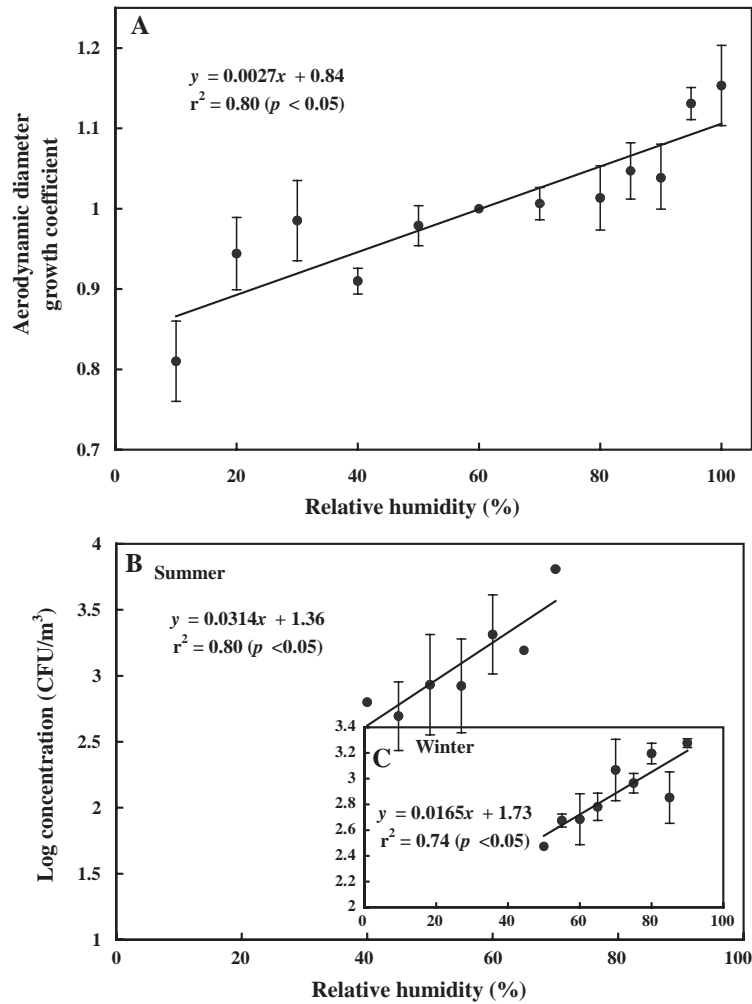


Fig. 3. The correction factor profiles of hygroscopic changes on aerodynamic diameter and concentration of airborne fungi: (A) a relative humidity-aerodynamic diameter growth coefficient profile and a relative humidity-concentration profile for (B) summer and (C) winter. The error bars represent one standard deviation from the mean.

We analyzed the available data from Lin and Li (1996) regarding the relationship between concentrations and RH to derive a region-specific seasonal variation RH-concentration profile in order to correct the indoor concentration of airborne fungi due to RH changes in northern Taiwan region (Fig. 3B). Fig. 3B shows that linear RH-concentration relationships prevailed for both summer and winter in that specific concentration correction factors due to RH in summer and in winter are $\log C_s(\text{RH}) = 0.0314 \text{ RH} + 1.36$ ($r^2 = 0.80$, $p < 0.05$) and $\log C_w(\text{RH}) = 0.0165 \text{ RH} + 1.73$ ($r^2 = 0.74$, $p < 0.05$), respectively. The concentration correction factor (RH_c), for example, in summer has the form as

$$\text{RH}_c = \frac{C_I(k') \left[\frac{C_s(\text{RH}_i)}{C_s(\text{RH}_0)} \right]}{C_I(k')} \quad (4)$$

The corrected indoor airborne fungal concentration, $C_i(k')$, in summer can be written as

$$C_i(k') = C_i(k') \times RH_c = \left(C_o(k') \frac{\lambda_n}{\lambda_n + \lambda_d(k')} \right) \left[\frac{C_s(RH_i)}{C_s(RH_o)} \right] \tag{5}$$

In this basic model, the impact of RH effect on airborne fungal concentration is almost completely captured by a simple expression for I/O ratio in the absent of indoor sources.

2.4. Fungal spores lung/indoor relationships

We divided HRT into five major compartments from the suggestion of ICRP66 (ICRP, 1994): (i) the nasal passage (ET₁), comprising the anterior nose and the posterior nasal passages; (ii) pharynx (ET₂), comprising larynx and mouth; (iii) the bronchial region (BB), comprising the airway from trachea, main bronchi, and intrapulmonary bronchi; (iv) the bronchiolar region (bb), comprising the bronchioles and terminal bronchioles; and (v) alveolar–interstitial region (AI), comprising the airway from respiratory bronchioli through alveolar sacs. Followed by the principle of mass balance, the dynamic equations of inspiratory oral cavity (IOC) varying with particle size range k and time t to each regional compartment are given a by a state-space realization form of a linear dynamic representation as (Liao et al., 2003; Chen et al., 2004),

$$\left\{ \frac{dC(k, t)}{dt} \right\} = [L(k)]\{C(k, t)\} + [B]\{u(k, t)\}, \tag{6}$$

where $\{C(k, t)\} = \{C_1(k, t), C_3(k, t), C_4(k, t), C_5(k, t)\}^T$ is the state variable vector of fungal spores concentrations in compartments ET₁, BB, bb, and AI, respectively, (CFU m⁻³); $\{u(k, t)\} = \{C_i(k, t) \ 0 \ 0 \ 0\}^T$ represents an input vector of fungal spores concentration (CFU m⁻³); $[L(k)]$ is the state matrix containing the essential parameters that describe the system characteristics (h⁻¹), and $[B]$ is the constant input matrix (h⁻¹).

Eq. (6) can be solved explicitly as fungal spore concentrations reach steady state. We define diagonal element in matrix $[L(k)]$ as L_{ii} and yield the fungal spore indoor–personal exposure relationships corresponding to fungal spore lung/indoor (L/I) ratio in each compartment as,

$$\frac{C_1(k)}{C_i(k)} = \frac{-\frac{Q}{V_1} \cdot \left(L_{33} \cdot L_{44} \cdot L_{55} - L_{33} \cdot \beta_{45} \frac{Q}{V_4} \beta_{54} \frac{Q}{V_5} - L_{55} \cdot \beta_{34} \frac{Q}{V_3} \cdot \beta_{43} \frac{Q}{V_4} \right)}{\|L(k)\|}, \tag{7a}$$

$$\frac{C_3(k)}{C_i(k)} = \frac{\frac{Q}{V_1} \cdot \beta_{31} \frac{Q}{V_3} \cdot \left(L_{44} \cdot L_{55} - \beta_{45} \frac{Q}{V_4} \cdot \beta_{54} \frac{Q}{V_5} \right)}{\|L(k)\|}, \tag{7b}$$

$$\frac{C_4(k)}{C_i(k)} = \frac{-\frac{Q}{V_1} \cdot \beta_{31} \frac{Q}{V_3} \cdot \beta_{43} \frac{Q}{V_4} \cdot L_{55}}{\|L(k)\|}, \tag{7c}$$

$$\frac{C_5(k)}{C_i(k)} = \frac{\frac{Q}{V_1} \cdot \beta_{31} \frac{Q}{V_3} \cdot \beta_{43} \frac{Q}{V_4} \cdot \beta_{54} \frac{Q}{V_5}}{\|L(k)\|}, \tag{7d}$$

Table 2

Rate equations of airborne fungi deposition for naturally ventilated airspace and for human respiratory tract (see Table 3 for description of symbols)

Naturally ventilated airspace

$$\lambda_d(k) = \frac{1}{d_{k+1} - d_k} \int_{d_k}^{d_{k+1}} \lambda_d(d_p) d(d_p) \tag{T-1}$$

where

$$\lambda_d(d_p) = \frac{1}{lwh} \left\{ (2wh + 2hl) \left(\left(\sin \frac{\pi}{n} \right) (k_e D(d_p)^{n-1})^{1/n} \right) + wlv_s(d_p) \coth \left(\frac{\pi v_s(d_p)}{2 \left(n \sin \frac{\pi}{n} \right) (k_e D(d_p)^{n-1})^{1/n}} \right) \right\} \tag{T-2}^a$$

$$D(d_p) = \frac{k_B TC_{slip}}{3\pi\eta_a d_p} \tag{T-3}^b$$

$$v_s(d_p) = \frac{\rho_p g d_p^2}{18\eta_a} C_{slip} \left(1 - \frac{\rho_a}{\rho_p} \right) \tag{T-4}^b$$

$$\text{Slip correlation factor : } C_{slip} = \left(1 + \frac{\lambda}{d_p} \left(2.541 + 0.8 \exp \left(-0.55 \frac{d_p}{\lambda} \right) \right) \right) \tag{T-5}^b$$

Human respiratory tract^c

$$\lambda_{d_1}(d_p) = \frac{8}{D_i} \sin \frac{\pi}{n} \left(k_e D(d_p)^{n-1} \right)^{1/n} \tag{T-6}^a$$

$$\lambda_{s_1}(d_p) = \frac{4v_s(d_p)}{D_i} \coth \left(\frac{\pi v_s(d_p)}{2 \left(n \sin \frac{\pi}{n} \right) (k_e D(d_p)^{n-1})^{1/n}} \right) \tag{T-7}^a$$

$$\lambda_{im_1}(d_p) = \frac{\rho_p d_p^2 C_{slip} g}{9\eta_a D_i} = Stk \frac{g}{U_i}, \quad \text{where } Stk = \text{Stokes number} \tag{T-8}^b$$

$$\varepsilon_i(d_p) = \frac{(1 - \alpha) \sum n_i \frac{d_p}{D_i}}{Ku \left(1 + \frac{d_p}{D_i} \right)} \tag{T-9}^b$$

$$\text{Kawabara number : } Ku = -\frac{\ln \alpha}{2} - \frac{3}{4} + \alpha - \frac{\alpha^2}{4} \tag{T-10}^b$$

^a Derived from Crump and Seinfeld (1981).

^b Adopted from Hinds (1999).

^c The integrated formula for the *k*th bin is the same as Eq. (T-1).

Table 3
A summary of input parameters appearing in model implementation

Parameter	Description	Representation values
<i>Lung physiological parameters^a</i>		
Q_f	Breathing frequency	15, 20 breaths min ⁻¹
V_t	Tidal volume	1.33, 3 L
C_L	Clearance rate by phagocyte	8.3×10^{-3} h ⁻¹
β_{ij}	Transfer coefficient between compartments i and j	0.9–1.1
D_1, D_2, D_3, D_4, D_5	Diameter of airways	0.5, 2.3, 1.2, 0.1, 0.05 cm
n_1, n_2, n_3, n_4, n_5	Number of airways	1, 1, 1, 6.5×10^4 , 4.5×10^7
V_1, V_2, V_3, V_4, V_5	Volume of compartments in lung	5.8, 82.1, 94.6, 510.2, 1580.4 cm ³
<i>Deposition rate parameters</i>		
n	Exponent constant	2.95 ^b
k_e	Turbulent intensity parameter	0.784 s ^{-1b}
k_B	Boltzmann's constant	1.38×10^{-16} dyn cm °C ^{-1c}
T	Ambient temperature	29 °C
η_a	Dynamic viscosity of air	1.85×10^{-4} g cm ⁻¹ s ^{-1c}
λ	Mean free path of air	0.66×10^{-5} cm ^c
ρ_a	Air density	1.18×10^{-3} g cm ^{-3c}
ρ_p	Particle density	1.0 g cm ^{-3c}

^a Adapted from ICRP66 (ICRP, 1994).

^b Adapted from Lai and Nazaroff (2000).

^c Adapted from Hinds (1999).

where $D_d(k', t)$ is the RH corrected time-dependent cumulative inhalation dose of fungal spores of each lung region in the k th size range (CFU); $C_i(k', t)$, $i=1,2,3,4,5$, is the time-dependent fungal spore concentration in lung region i in the k th size range; and $d_F(k)$ is the fungal spores deposition fraction of each lung region in the k th size range and has the form as,

$$d_F(k') = \frac{C_i(k')}{C_1(k')} \left[(\lambda_{d_i}(k') + \lambda_{s_i}(k') + \lambda_{im_i}(k')) \cdot \frac{V}{Q} + \varepsilon_i(k') \right]. \quad (10)$$

The differences in exposure can vary due to factors such as diameter of airways, breathing rate, fungal spores profile, and time spent in the homes. The time-dependent size distribution of fungal spores from the dynamic model of Eq. (6) was combined with inhalation dose model (Eq. (10)) for the size-dependent dose to obtain the integrated inhalation dose, as a function of particle size in that we assumed RH in HRT was 100%.

2.7. Addressing uncertainty

Because of limitations in the data and theories to support airborne fungi indoor/outdoor/lung modeling in naturally ventilated airspace, there is a need to characterize uncertainty and variability in the model approach and input parameters. We used the essential data of Lin and Li (1996) and a Monte Carol simulation to quantify our certainty concerning airborne fungi indoor/outdoor/lung (I/O/L) ratio attributable to outdoor airborne fungal concentration, natural ventilation rate, and RH correction factors. We employed the K–S statistics to optimize the goodness-of-fit of distributions. We employed @RISK (Version 4.5, Professional Edition, Palisade Corp., USA) to analyze data and to estimate distribution parameters. Results from goodness-of-fit statistics suggest that the normal distribution model fits optimally the observed data. For this study, 5000 iterations are sufficient to ensure stability of results.

3. Results and discussion

3.1. Fungal spores I/O relationships

The particle size distributions of airborne fungi in indoor and outdoor are shown in Fig. 4A–H in that airborne fungi in summer have higher indoor/outdoor concentrations than that in winter at selected time periods. There were major temperature and RH fluctuations being observed in winter ($\Delta RH = 16.59 \pm 2.63\%$ in winter ($RH_o > RH_i$), and $9.94 \pm 6.63\%$ in summer ($RH_o < RH_i$); $\Delta T = 4 \pm 0.7^\circ\text{C}$ in winter ($T_o < T_i$), and $3 \pm 2^\circ\text{C}$ in summer ($T_o > T_i$)) (Fig. 1C, D, E) result in a larger difference in outdoor/indoor airborne fungal concentrations than that in summer. Generally in winter, a large portion of the airborne fungal concentrations is removed (Fig. 4E–H), indicating that both deposition and air exchange are efficient removal mechanisms, yet this phenomenon does not occur in summer.

The predicted indoor airborne fungal concentrations are presented in Fig. 4I and J in that box and whisker plots are used to represent uncertainty. The predicted mean values all fall within the interquartile. The higher indoor airborne fungal concentrations occurred in early and late afternoon in which median values were 699.29 and 626.20 CFU m^{-3} at 2 am and 8 pm, respectively, in summer; whereas 138.71 and 99.01 CFU m^{-3} at 2 am and 8 pm, respectively, in winter. Fig. 4I indicates that the 95th-percentile predictions of indoor airborne fungal concentration in summer are far above 1000 CFU m^{-3} at 2 am and 8 pm, indicating the indoor environment may be in need of investigation and improvement (Morey et al., 1984). The variation in the total airborne fungal concentrations at 2 pm was lower than that at other time periods for both summer and winter. Strength of higher indoor airborne fungal concentrations in summer is partly explained by higher outdoor concentrations (Fig. 1F), higher slope of the fitted relationships between concentration and RH in summer (Fig. 3B), and lower air exchange rate (AER) (in summer: $AER = 0.008 \pm 0.0027$ s^{-1} ; in winter $AER = 0.010 \pm 0.0036$ s^{-1}). Little studies containing suitable data were identified, thus extremely limited empirical evidence was available for model validation, especially for the wind-induced naturally residences in Taiwan region.

Our results also reveal that the average GMDs airborne fungi decrease from outdoor 2.58 ± 0.37 μm to indoor 1.91 ± 0.12 μm in summer, whereas decrease from outdoor 2.79 ± 0.32 μm to indoor 1.73 ± 0.10 μm in winter. The results suggest that the hygroscopicity of airborne fungi as a function of RH significantly affect their AED, and thus change their deposition pattern in a wind-induced naturally ventilated airspace (Reponon et al., 1996; Chen et al., 2003; Kemp et al., 2003). Airborne fungal concentrations in indoor environments also vary with the amount of mechanical and/or human activity. Large numbers of people or abundant activity stirs up dust that reentraining settled spores and intensifies air currents, delaying deposition by gravity. Wickman et al. (1992) has been used the house dust as a surrogate for airborne exposure to fungi, indicating no direct connection between results of house dust analyses and respiratory symptoms, yet high CFUs from house dust were associated with higher RH.

With these finding, one could expect to encounter a fairly high concentration of airborne fungi during the morning and the indoor RH remained at the range between 65–75%. It is alarming for those occupants who were likely to develop some hypersensitive diseases. Although the natural ventilation system was observed to be capable of reducing the airborne fungal concentrations to a relative low concentrations comparing with the outdoor concentrations, occupants working during this period were exposed to a high risk of respiratory system infection. Our results also indicate that the airborne fungal concentrations showed to have no significant relationship with the average RH in the previous 6 h, although the concentration of airborne fungi always found to be the highest in the morning. The results also demonstrate that if there were no major interference caused by the people activities, the daily indoor airborne fungal concentration would appear in a similar profile.

Fig. 5A depicts the size-dependent indoor airborne fungal concentrations varied with seasonality and temporality. Recently very few measurements were conducted to evaluate size distributions of airborne fungi in indoor atmosphere. Our present research found that the maximum concentrations of the indoor airborne fungal concentrations occurred in the size range of 0.65 – 2.5 μm AED (Fig. 5A). Lin and Li (1996) indicated that large numbers of outdoor fungus

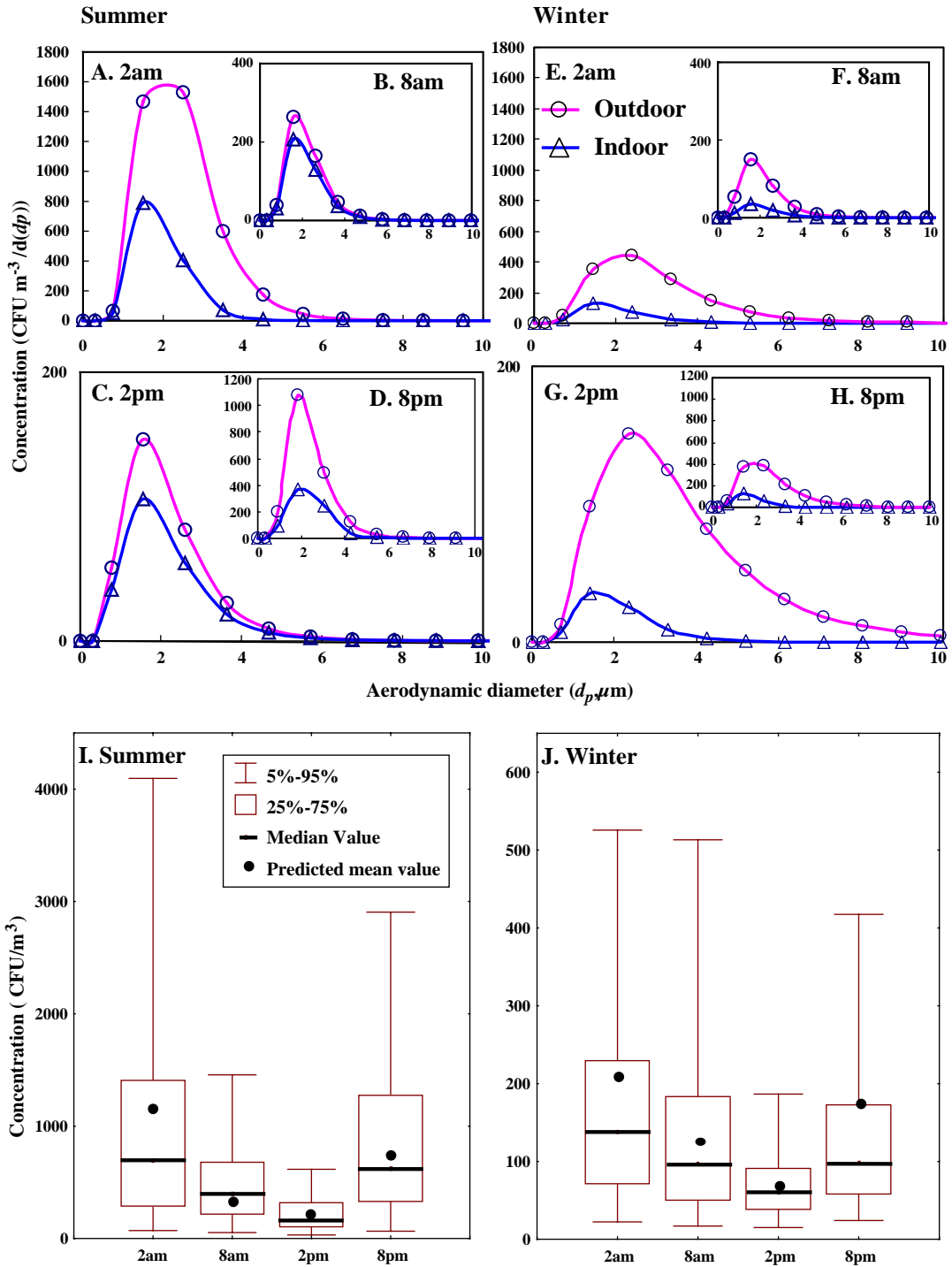


Fig. 4. (A–H) The temporal/seasonal variations of particle size distribution of airborne fungal concentrations in outdoor (○) and indoor (△), and box and whisker plot presentations of predicted indoor airborne fungal concentrations in (I) summer and in (J) winter at certain time periods.

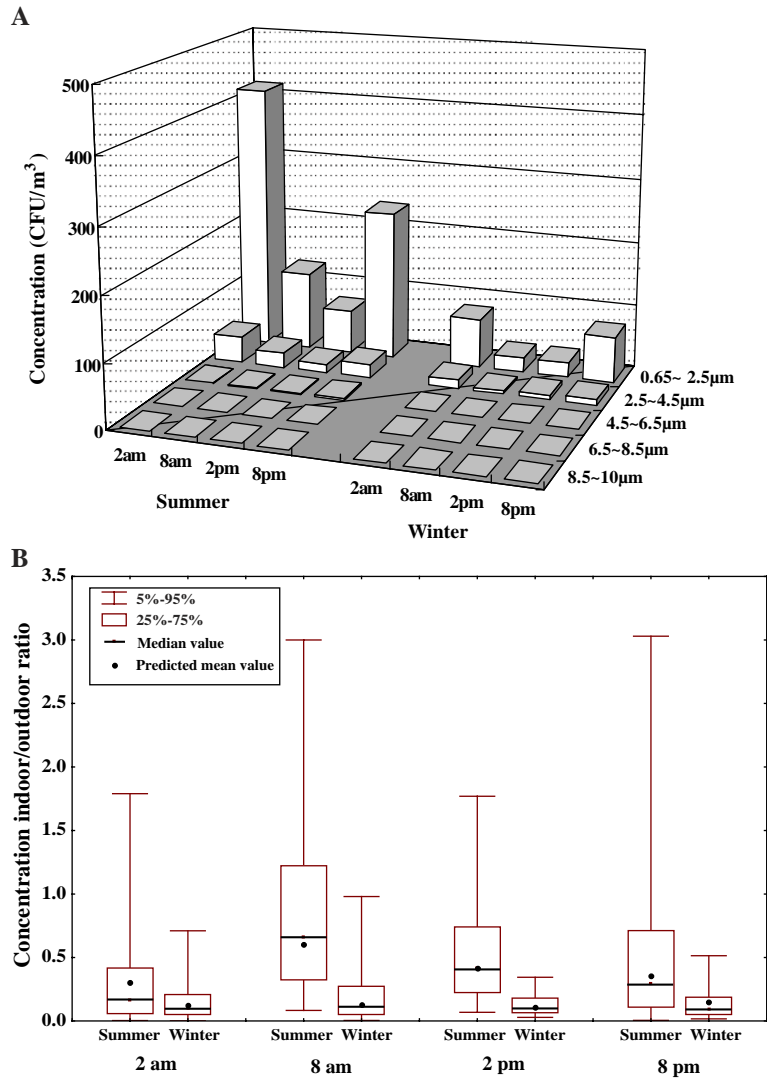


Fig. 5. (A) The temporal/seasonal variations of indoor airborne fungal concentrations in different size ranges and (B) the temporal/seasonal variations of calculated concentration I/O ratios of airborne fungi.

spores isolated were found to be in the size range of 2.1–3.3 μm with a GMD in the size range of 1.96–3.40 μm. Reponon et al. (1996) pointed out that for bioaerosol particles, ranging from 0.1 to 10 μm in diameter, the greatest change in the respiratory deposition due to hygroscopic size changes occurs in the particles size range of 0.5–2 μm.

In the absence of indoor sources of bioaerosol, summer has higher I/O ratios of airborne fungal concentration (mean ranging from 0.29 to 0.58) than

that in winter (mean ranging from 0.12 to 0.16; Fig. 5B). Fig. 5B shows that the variation in the concentration I/O ratio for summer was higher than that in winter partly due to the variation of outdoor concentrations in summer is greater than that in winter (Fig. 1F). The 95th percentile I/O ratios are all greater than 1 in summer, whereas in winter all 95th percentile I/O ratios are less than 1. Generally, the I/O ratios of interquartile are all less than 1. To identify the potential fungal reservoir, Su et al. (2001) suggested

that I/O comparisons were used to document the presence of biologically derived contamination. Su et al. (2001) further indicated that, in southern Taiwan region homes, the I/O ratios of *Cladosporium* spp., *Aspergillus* spp., *Penicillium* spp., *Alternaria* spp. and yeast were often lower than 1, whereas more than 60% and 62.9% of investigated homes gave I/O ratios of *Cladosporium* spp. and *Alternaria* spp. lower than 1 in very season and in spring/winter, respectively. Su et al. (2001) also indicated that a significantly correlation between indoor and outdoor airborne fungal concentrations. Wu et al. (2000) had evaluated the airborne fungal concentrations in urban and suburban homes with natural ventilation and the results showed that the I/O ratios of total airborne fungal concentrations were 0.766 and 0.908 in winter, whereas 0.873 and 1.170 in summer for urban and suburban homes, respectively.

The most predominant fungal concern from indoor source is *Penicillium* spp. for winter and *Aspergillus* spp. for summer in Taiwan region (Kuo and Li, 1994; Li et al., 1995; Wu et al., 2000). *Aspergillus* spp. is a mycotoxin-producing genus and *Penicillium* spp. is reported to be associated with many hypersensitivity diseases. Parsimoniously, our present bioaerosol I/O model can be used to derive the indoor source concentrations provided that the actual measured fungus-specific I/O ratios are available. Here we employed our predicted average I/O ratio ($=C_i/C_o$) of 0.41 in summer to estimate the indoor source concentration in a suburban home in which the actual measured average I/O ratio ($=(C_i+C_s)/C_o$, where C_s is the indoor source concentration) of total fungi is 1.17 (Wu et al., 2000), resulting $C_s=0.76C_o=0.76\times 6241.65$ CFU $m^{-3}=4743.65$ CFU m^{-3} and indoor airborne fungal concentration that attributable to outdoor is equal to $C_i=7302.70-4743.65=2559.05$ CFU m^{-3} .

3.2. Fungal spores L/I relationships

The fungal concentration distribution patterns in different lung regions have no significant temporal variation, yet have a different concentration resulted from the indoor fungal concentrations in summer (Fig. 6A). Fig. 6A also indicates that the higher lung fungal concentrations occurred in early morning (2 am) and late afternoon (8 pm). Because the airborne fungal

concentrations within the five compartments reach the steady state in 5–10 sec for all the size ranges, it is more important to understand the fungal concentration L/I ratio, deposition fraction, and inhale exposure dose than the dynamics of airborne fungi in HRT. Comparing the concentrations in ET₁ with AI compartments, the deeper lung region has a lower fungal concentration as a result of the deposition makes the fungi no longer airborne especially in bigger size range (Fig. 6A).

The lung ET₁ has higher fungal L/I ratios (0.7–0.8) than that of lung regions BB (0.41–0.60), bb (0.12–0.40), and AI (0.01–0.24), whereas the distribution patterns of the size-dependent L/I ratios decreasing with the size range are similar in lung regions (Fig. 6B). Generally, the region AI has higher fungal deposition rates (95th percentile is 0.22 CFU s^{-1} at 2 am) than that of in regions ET₁/BB (95th percentile <0.05 CFU s^{-1} at 2 am) and bb (95th percentile is 0.13 CFU s^{-1} at 2 am; Fig. 7). On a daily basis, the highest airborne fungal deposition dose occurred in 11 pm–05:00 am in lung region AI (95th-percentile is 4600 CFU) in that AI region has higher fungal deposition dose than that of regions ET₁/BB/bb (Fig. 8A). Fig. 8B shows that 95th-percentile predictions of daily airborne fungal dose rate are 1000, 6000, 230, and 58 CFU day^{-1} , respectively, in regions AI, bb, BB, and ET₁. The airways of AI compartment has an extremely large wall surface than that in lung regions ET₁, BB, and bb, it makes the magnitude of fungi deposition CFU dose on the wall much higher in AI than that in other lung regions.

For relative high-temperature differences larger than 20 °C, thermophoresis has a pronounced effect on the size distribution evolution, enhancing deposition along the airways (Lazaridis et al., 2001). Thermophoretic deposition of airborne fungi in HRT is not considered in this work due to the temperature differences within 7 °C between airway wall (assuming a constant temperature of 36 °C) and indoor ambient space (the measured temperature is 29 °C). The thermophoresis is neglected not only due to a relative small temperature difference but also due to the smaller effect compared with the other deposition mechanisms, e.g. inertial impaction and gravitational settling (Hinds, 1999). Airborne fungi undergo hygroscopic growth in the high RH environment of HRT. Therefore, when the airborne fungi entering the

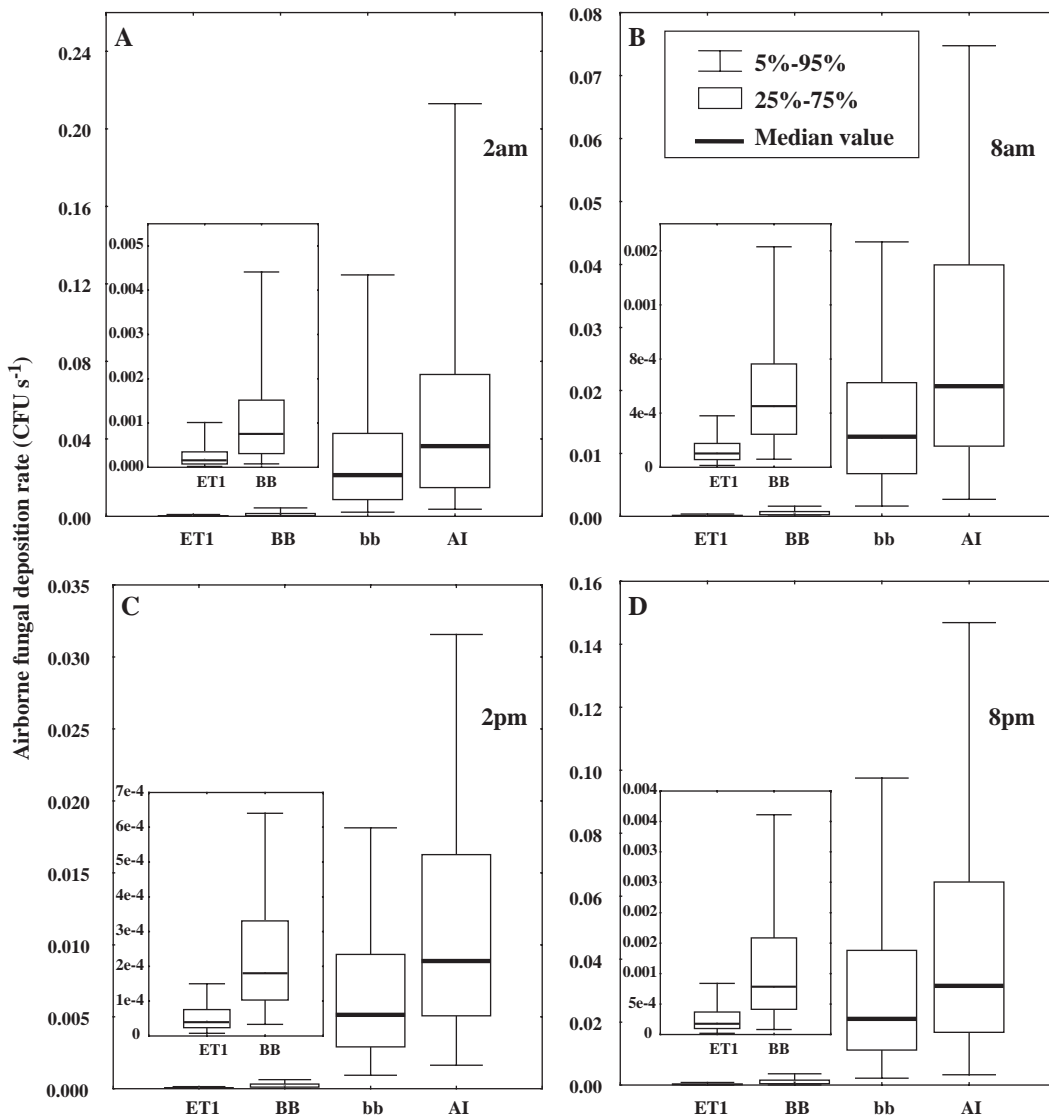


Fig. 7. Box and whisker plot representations of airborne fungal deposition rates in different HRT regions at (A) 2 am, (B) 8 am, (C) 2 pm, and (D) 8 pm.

lung, the amount of possible growth depends on how close the RH indoors is to 100% and further alters the deposition patterns within the lung. We have incorporated hygroscopic growth effects into our model simulations.

Our proposed simple lung model provides an easy yet robust way to account for and keep track of the contribution of different processes of lung deposition profiles, even though our model is based on many

idealized assumptions such as one-dimensional air-flow and single morphological change. Our approach can also examine independently the processes and mechanisms that govern the inhalation route of the exposure–dose–response scenario.

As the detailed background bioaerosol level and some indoor parameters were measured, the human exposure characteristics on bioaerosol may be able to be formulated through a mathematical model. This

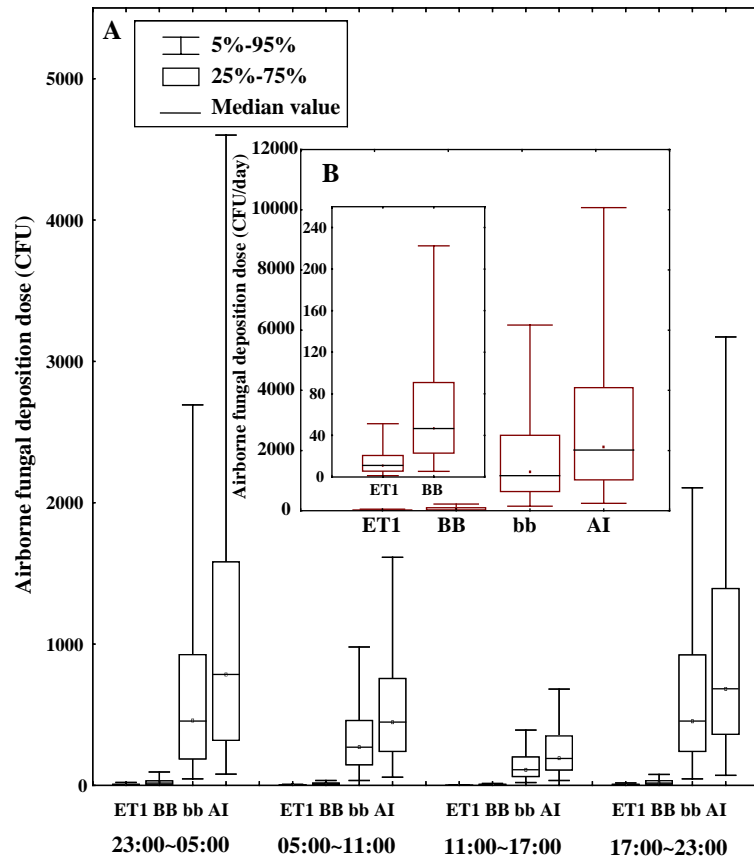


Fig. 8. Box and whisker plot representations of (A) airborne fungal deposition dose in different HRT regions at certain time period and (B) daily airborne deposition dose rates in different HRT regions.

should be much easier and cost effective to do so as compared with the continuous bioaerosol measurement. This information needs to be correlated with outdoor spore concentrations, with indoor environmental conditions, with the types of ventilation systems, with the building types, and with instances of respiratory disease.

4. Conclusions

We have coupled a simple well-defined size-dependent indoor air quality approach with a compartmental lung model in conjunction with a hygroscopic growth factor as a function of relative humidity in aerodynamic diameter and concentration of fungal spores to estimate the indoor/outdoor/personal expo-

sure relationships of airborne fungal concentration for a wind-induced naturally ventilated home in Taiwan region. We have successfully employed the published data including seasonal/temporal outdoor airborne fungi size characteristics and meteorological information such as wind direction/speed, temperature, and relative humidity to characterize the contribution of outdoor fungi to residential exposures.

We have further confirmed the robustness of the estimates by using Monte Carlo simulations based on the observed distributions of critical parameters from our proposed model. These methods capture in simple distributions such complexities as indoor air mixing patterns, heterogeneity of indoor sources of fungal spores, and the effects of seasonality on outdoor size characteristics of airborne fungal spores. Such simplifications allow us to measure the relative impact of

a number of specific factors, such as the contributions of indoor sources, airborne fungi deposition mechanism, human exposure, and the effective methods for exposure control. Our results demonstrate the importance of knowing the information of temporal/seasonal- and particle size distribution of outdoor bioaerosol for understanding residential exposure to airborne fungi of outdoor origin. More importantly, this research illustrates that an exposure assessment based on total bioaerosol measured outdoors may obscure the actual causal relationships to indoor fungal spores of outdoor origin.

Future work should certainly focus on quantifying indoor aerobiology of airborne fungi and other environmental parameters in a variety of circumstances. On the other hand, we may use fungus-specific parameters to conduct more detailed models of transport changes in airborne fungi from outdoor to indoor air that realistically incorporate the effects of heterogeneities in specific settings.

Acknowledgments

The authors wish to acknowledge the financial support of the National Science Council of the Republic of China under Grant NSC 92-2313-B-002-103.

References

- Abt E, Suh HH, Catalano P, Koutrakis P. Relative contribution of outdoor and indoor particle sources to indoor concentrations. *Environ Sci Technol* 2000;34:3579–87.
- Burge HA, Chew G, Muilenberg M, Gold BL. Role of fungi in-house dust ecosystems. *J Allergy Clin Immunol* 1995;95:167.
- Chen LY, Jeng FT, Chen CC, Hsiao TC. Hygroscopic behavior of atmospheric aerosol in Taipei. *Atmos Environ* 2003;37:2069–75.
- Chen JW, Liao CM, Chen SC. Compartmental human respiratory tract modeling of airborne dust exposure from feeding in swine buildings. *J Air Waste Manage Assoc* 2004;54:331–41.
- Crump JG, Seinfeld JH. Turbulent deposition and gravitational sedimentation of an aerosol in a vessel of arbitrary shape. *J Aerosol Sci* 1981;12:405–15.
- Hinds WC. *Aerosol technology: properties, behavior, and measurement of airborne particles*. 2nd ed. New York: John Wiley; 1999.
- Huang CY, Lee CC, Li FC, Ma YP, Su HJJ. The seasonal distribution of bioaerosols in municipal landfill sites: a 3-yr study. *Atmos Environ* 2002;35:4385–95.
- Hyvärinen A, Vahteristo M, Meklin T, Jantunen M, Nevalainen A, Moschandreas D. Temporal and spatial variation of fungal concentrations in indoor air. *Aerosol Sci Tech* 2001;35:688–95.
- ICRP. Human respiratory tract model for radiological protection, a report of a task group of the International Commission on Radiological Protection. ICRP Publication, vol. 66. New York: Elsevier; 1994.
- Johnson DL, Pearce TA, Esmen NA. The effect of phosphate buffer on aerosol size distribution of nebulized *Bacillus subtilis* and *Pseudomonas Fluorescens* bacteria. *Aerosol Sci Tech* 1999;30:202–10.
- Kemp PC, Neumeister-Kemp B, Lysek G, Murray F. Changes in airborne fungi from the outdoors to indoor air: large HVAC systems in nonproblem buildings in two different climates. *AIHA J* 2003;64:269–75.
- Koblinger L, Hofmann W. Monte-Carlo modeling of aerosol deposition in human lungs: 1. Simulation of particle transport in a stochastic lung structure. *J Aerosol Sci* 1990;21:661–74.
- Kuo YM, Li CS. Seasonal fungus prevalence inside and outside of domestic environments in the subtropical climate. *Atmos Environ* 1994;28:3125–30.
- Lai AK, Nazaroff WW. Modeling indoor particle deposition from turbulent flow onto smooth surfaces. *J Aerosol Sci* 2000;31:463–76.
- Law AKY, Chau CK, Chan GYS. Characteristics of bioaerosol profile in office buildings in Hong Kong. *Build Environ* 2001;36:527–41.
- Lazaridis M, Brody DM, Hov O, Georgopoulos PG. Integrated exposure and analysis systems: 3 Deposition of inhaled particles in the human respiratory tract. *Environ Sci Technol* 2001;35:3727–34.
- Lee BK, Kim SH, Kim SS. Hygroscopic growth of *E coli* and *B subtilis* bioaerosols. *J Aerosol Sci* 2002;33:1721–3.
- Li CS, Hsu LY, Chou CC, Hsieh KH. Fungus allergens inside and outside the residences of atopic and control children. *Arch Environ Health* 1995;50:38–43.
- Li CS, Hsu CW, Chua KY, Hsieh KH, Lin RH. Environmental distribution of house dust mite allergen (*Der p 5*). *J Allergy Clin Immunol* 1996;97:857–9.
- Liao CM, Chen JW, Huang SJ. Size-dependent PM₁₀ indoor/outdoor/personal relationships for a wind-induced naturally ventilated airspace. *Atmos Environ* 2003;37:3065–75.
- Lin WH, Li CS. Size characteristics of fungus allergens in the subtropical climate. *Aerosol Sci Technol* 1996;25:93–110.
- Madelin TM, Johnson HE. Fungal and actinomycete spore aerosols measured at different humidities with an aerodynamic particle sizer. *J Appl Bacteriol* 1992;72:400–9.
- Meklin T, Reponen T, Toivola M, Koponen V, Husman T, Hyvärinen A, et al. Size distributions of airborne microbes in moisture-damaged and reference school building of two construction types. *Atmos Environ* 2002;36:6031–9.
- Morey PR, Hodgson MJ, Sorenson WG, Kullman GH, Rhodes GS, Visvesvara GS. Environmental studies in moldy office buildings: biological agents, sources and preventive measures. Annual American Conference of Governmental Industrial Hygienists, Cincinnati, OH, 1984.

- Pasanen AL, Pasanen P, Jantunen MJ, Kalliokoski P. Significance of air humidity and air velocity for fungal spore release into the air. *Atmos Environ* 1991;25A:459–62.
- Reponen T, Willeke K, Ulevicius V, Reponen A, Grinshpun SA. Effect of relative humidity on the aerodynamic diameter and respiratory deposition of fungal spores. *Atmos Environ* 1996;30:3967–74.
- Riley WJ, McKone TE, Lai AK, Nazaroff WW. Indoor particulate matter of outdoor origin: importance of size-dependent removal mechanisms. *Environ Sci Technol* 2002;36:1868.
- Su HJ, Wu PC, Chen HL, Lee FC, Lin LL. Exposure assessment of indoor allergens, endotoxin, and airborne fungi for homes in southern Taiwan. *Environ Res* 2001;85:135–44.
- Su HJJ, Chen HL, Huang CF, Lun CY, Li FC, Milton DK. Airborne fungi and endotoxin concentrations in different areas within textile plants in Taiwan: a 3-year study. *Environ Res* 2002;89:58–65.
- Wickman M, Gravesen S, Nordvall SL, Pershagen G, Sundell J. Indoor viable dust-bound microfungi in relation to residential characteristics, living habits, and symptoms in atopic and control children. *J Allergy Clin Immunol* 1992;89:752.
- Wu PC, Su HJ, Lin CY. Characteristics of indoor and outdoor airborne fungi at suburban and urban homes in two seasons. *Sci Total Environ* 2000;253:111–8.
- Yu H, Hou CH, Liao CM. Scale model analysis of opening effectiveness for wind-induced natural ventilation openings. *Biosyst Eng* 2002;82:199–207.